

Numerical Method

The flow between two symmetrically spaced wedges was simulated. When it was assumed that viscous effects on the interaction of shock waves generated by the wedges were negligible, the unsteady Euler equations were solved. The perfect gas model with $\gamma = 1.4$ was used. The simulations were performed with a shock-capturing total variation diminishing (TVD) scheme. The fourth-order formula was utilized to reconstruct cell face values of the primitive variables (the density, the pressure, and the velocity components) from cell-averaged ones. Numerical fluxes were calculated by the Harten–Lax–van Leer–Einfeldt (HLLC) approximate Riemann solver, which is very robust for modeling high-speed flows. Time integration was accomplished by the third-order explicit TVD Runge–Kutta scheme. A more detailed description of the numerical techniques may be found in Ref. 14.

Because of the symmetry of the problem, the computations were performed only in one-half of the domain (Fig. 2). The length of the inclined section of the wedge surface is w , and the distance from the trailing edge of the wedge to the plane of symmetry is g . The ratio g/w was chosen to be 0.42. This value meets two conditions: The incident shock wave does not interact with the expansion fan emanating from the trailing edge of the wedge, and the reflected shock wave does not impinge on the wedge surface. The computational domain was divided approximately into 60,000 quadrilateral cells. A uniform supersonic flow was specified on the left (inflow) boundary of the domain and the zero-order extrapolation was employed on the right (outflow) boundary. The bottom boundary was treated as a plane of symmetry, and solid wall conditions were imposed on the top boundary.

The inflow Mach number was varied by changing the boundary conditions. The inflow pressure and density were kept constant while the velocity was changed so that an increment of the flow Mach number was equal to 0.05. As a result, weak disturbances were formed on the left boundary. They moved downstream and interacted with the shock reflection configuration. The solution was integrated in time until this unsteady transient process was completed, and the flow reached a steady state. After that, the flow Mach number was changed again.

To ensure the independence of the results on the grid resolution, some of the computations were repeated with finer grids (up to

160,000 cells). The agreement between the coarse and fine grid results was excellent.

Numerical Results

Both the $\theta_w > \theta_{w,\max}^N$ and $\theta_w < \theta_{w,\max}^N$ cases were considered. Typical results for the former are shown in Fig. 2. The wedge angle was kept constant during the simulation at $\theta_w = 27^\circ > \theta_{w,\max}^N = 20.92^\circ$ while the flow Mach number was first decreased from 5 to 4.45 and then increased back to 5. Figure 2, frame 1, shows an RR, with $M = 5$, inside the dual-solution domain. As M was reduced, the detachment transition line beyond which an RR is theoretically impossible was reached at $M = 4.57$. The RR \rightarrow MR transition took place when the flow Mach number was changed from 4.5 to 4.45 (Fig. 2, frames 3 and 4). Based on these two frames, the transition occurred at $M = 4.475 \pm 0.025$, in reasonable agreement with the theoretical value of $M = 4.57$. The existence of an RR slightly beyond the theoretical limit has been also observed in many numerical simulations of the wedge-angle variation-induced hysteresis and can be explained by the influence of numerical viscosity inherent in any shock-capturing code. Once MR was established, the flow Mach number was increased up to its initial value $M = 5$. Because theoretically an MR can exist for values of M inside the dual-solution domain, the reversed MR \rightarrow RR transition did not take place at the detachment line. As a result, two different stable wave configurations, an RR and an MR, were obtained inside the dual-solution domain for identical flow conditions, that is, M and ϕ or θ_w . This can clearly be seen in Fig. 2 by comparing the pairs of frames 1 and 7, 2 and 6, and 3 and 5 in which the first frame is an RR and the second one is an MR, respectively.

The second series of simulations was performed at $\theta_w = 20.5^\circ < \theta_{w,\max}^N = 20.92^\circ$. For this value of θ_w , the Mach number values that correspond to the von Neumann criterion are 3.47 and 6.31, whereas that corresponding to the detachment criterion is 2.84. The Mach number was decreased from $M = 3.5$ to 2.8, and then increased up to the initial value. Some frames showing the sequence of events are given in Fig. 3. The RR \rightarrow MR transition occurs between $M = 2.9$ and 2.8, in close agreement with the theoretical value, whereas the reverse, MR \rightarrow RR transition, is observed between $M = 3.2$ and 3.3, that is, slightly earlier than that predicted theoretically. This disagreement can be attributed to the very small height of

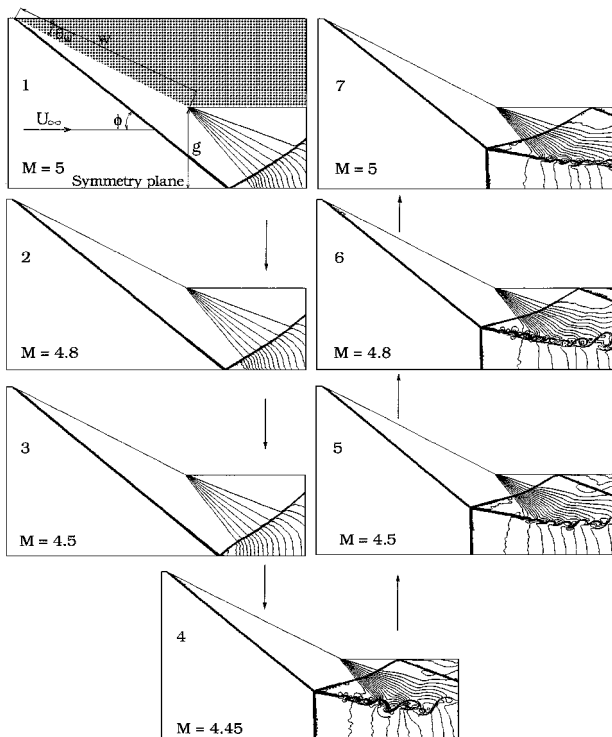


Fig. 2 Numerical frames (constant density contours) illustrating shock wave reflection transitions during variation of the flow Mach number at constant $\theta_w = 27^\circ$.

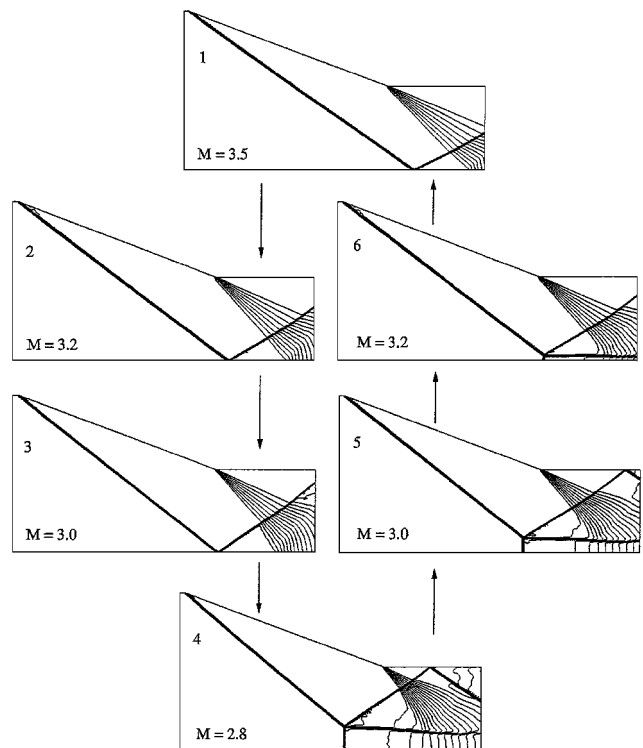


Fig. 3 Numerical frames (constant density contours) illustrating shock wave reflection transitions during variation of the flow Mach number at constant $\theta_w = 20.5^\circ$.

the Mach stem near the von Neumann criterion, which makes its numerical resolution very difficult. Figure 3 demonstrates clearly the existence of the flow Mach number variation-induced hysteresis.

Conclusions

It was shown numerically that, in addition to the wedge-angle variation-induced hysteresis in the RR \leftrightarrow MR transition, which was first illustrated numerically in Ref. 10, a flow Mach number variation-induced hysteresis is also possible in two-dimensional steady flows. For the latter, two different shock wave reflection configurations can be obtained at the same values of angle of incidence and flow Mach number, depending on the direction from which the flow Mach number was reached.

Because the investigated geometry resembles the geometry of supersonic intakes, the new hysteresis type that is reported in the present study can be relevant to flight performance at high supersonic speeds. The possible dependence of the flow pattern on the preceding maneuvers of an aircraft should be taken into account in designing intakes for perspective hypersonic vehicles.

Acknowledgment

The Russian authors of this Note would like to acknowledge the support of the Russian Foundation for Basic Research, Grant 00-01-00824.

References

- ¹Ben-Dor, G., *Shock Wave Reflection Phenomena*, Springer-Verlag, New York, 1991, Chap. 3.
- ²Von Neumann, J., "Oblique Reflection of Shocks," Navy Dept., Explosive Research Rept. 12, Bureau of Ordnance, Washington, DC, 1943 (reprinted in *Collected Works of J. von Neumann*, Vol. 6, Pergamon, Oxford, 1963, pp. 238–299).
- ³Hornung, H. G., Oertel, H., Jr., and Sandeman, R. J., "Transition to Mach Reflection of Shock Waves in Steady Flow With and Without Relaxation," *Journal of Fluid Mechanics*, Vol. 90, 1979, pp. 541–560.
- ⁴Hornung, H. G., and Robinson, M. L., "Transition from Regular to Mach Reflection of Shock Waves. Part 2. The Steady Flow Criterion," *Journal of Fluid Mechanics*, Vol. 123, 1982, pp. 155–164.
- ⁵Henderson, L. F., and Lozzi, A., "Further Experiments on Transition to Mach Reflection," *Journal of Fluid Mechanics*, Vol. 94, 1979, pp. 541–559.
- ⁶Teshukov, V. M., "On Stability of Regular Reflection of Shock Waves," *Prikladnaya Mekhanika i Technicheskaya Fizika (Applied Mechanics and Technical Physics)*, No. 2, 1989, pp. 26–33 (in Russian).
- ⁷Li, H., and Ben-Dor, G., "Application of the Principle of Minimum Entropy Production to Shock Wave Reflections. I. Steady Flows," *Journal Applied Physics*, Vol. 80, 1996, pp. 2027–2037.
- ⁸Chpoun, A., Passerel, D., Li, H., and Ben-Dor, G., "Reconsideration of the Oblique Shock Wave Reflection in Steady Flows. I. Experimental Investigation," *Journal of Fluid Mechanics*, Vol. 301, 1995, pp. 19–35.
- ⁹Vuillon, J., Zeitoun, D., and Ben-Dor, G., "Reconsideration of the Oblique Shock Wave Reflection in Steady Flows. I. Experimental Investigation," *Journal of Fluid Mechanics*, Vol. 301, 1995, pp. 37–50.
- ¹⁰Ivanov, M. S., Gimelshein, S. F., and Beylich, A. E., "Hysteresis Effect in Stationary Reflection of Shock Waves," *Physics of Fluids*, Vol. 7, 1995, pp. 685–687.
- ¹¹Li, H., Chpoun, A., and Ben-Dor, G., "Analytical and Experimental Investigations of the Reflection of Asymmetric Shock Waves in Steady Flow," *Journal of Fluid Mechanics*, Vol. 390, 1999, pp. 25–43.
- ¹²Ben-Dor, G., "Hysteresis Phenomena in Shock Wave Reflections in Steady Flows," *Proceedings of 22nd International Symposium on Shock Waves*, Vol. 1, edited by G. J. Ball, R. Hillier, and G. T. Roberts, Univ. of Southampton, Southampton, England, U.K., 1999, pp. 49–56.
- ¹³Onofri, M., and Nasuti, F., "Theoretical Considerations on Shock Reflections and Their Implications on the Evaluations of Air Intake Performance," *Proceedings of 22nd International Symposium on Shock Waves*, Vol. 2, edited by G. J. Ball, R. Hillier, and G. T. Roberts, Univ. of Southampton, Southampton, England, U.K., 1999, pp. 1285–1290.
- ¹⁴Khotyanovsky, D. V., Kudryavtsev, A. N., and Ivanov, M. S., "Numerical Study of Transition Between Steady Regular and Mach Reflection Caused by Free-Stream Perturbations," *Proceedings of 22nd International Symposium on Shock Waves*, Vol. 2, edited by G. J. Ball, R. Hillier, and G. T. Roberts, Univ. of Southampton, Southampton, England, U.K., 1999, pp. 1261–1266.

P. Givi

Associate Editor

Influence of External Caps on the Dynamic Behavior of Aerospace Cylindrical Vessels

Silvano Tizzi*

University of Rome "La Sapienza," 00184 Rome, Italy

Introduction

A MORE complete structural numerical simulation model than the one utilized in a previous work¹ for the dynamic analysis of cylindrical tanks is necessary for the analysis of the dynamic behavior of vessel structures with axisymmetric caps at the ends, which can be applied to generic axisymmetric shells of revolution.

Flügge² introduced a simplified linear model for static and dynamic behavior of axisymmetric thin shells (also see Ref. 3). Narasimhan and Alwar⁴ utilized the same model for a study of vibration of orthotropic spherical shells and introduced an interesting numerical procedure based on the Chebyshev–Galerkin spectral method for the evaluation of free vibration frequencies and modal shapes.

Hwang and Foster utilized a similar and simpler model for a study of the dynamic behavior of isotropic shallow spherical shells with a circular hole,⁵ but the out-of-plane shear behavior and rotary inertia were not taken into account. They found a solution of the free vibrational frequency equation in terms of Bessel functions and modified Bessels functions.

Ozakca and Hinton⁶ built a Mindlin⁷–Reisner⁸ axisymmetric finite element model with the same kinematic relations, where the out-of-plane and rotary inertia effects with varying shell thickness are taken into account, for a free vibration analysis and optimization of axisymmetric shells of revolutions.

As in the previous work,¹ a simplified numerical model for the dynamic analysis of an orthotropic antisymmetric angle-ply laminated axisymmetric shell has been developed here. The considered structure is the same as the one dealt with by Mizusawa and Kito,⁹ who utilized the first-order shear deformation Sanders' shell theory to analyze the vibration behavior. An out-of-plane shear stress distribution along the thickness coordinate according to the Mindlin⁷–Reisner⁸ theory is imposed. The same kinematic relations utilized by the mentioned authors,^{1–5} with appropriate approximations, have been employed to build this structural model.

A numerical procedure,^{1,10–13} which lies between the Rayleigh–Ritz method (see Refs. 14 and 15) and the finite element method (FEM)^{3,16,17} and which is obtained by combining the Ritz analysis with the variational principles,^{18–20} has been applied to find the free frequencies and vibration modes.

We have seen in the whole cylindrical structure case that there are low-frequency (lf) vibrating modes, flexural and flexural-torsional (FT) modes, and high-frequency (hf) shear vibration modes, where the displacements can be neglected with respect to the rotations: These can be divided into shear-flexural (SF) modes, where the rotation ϕ_s is predominant with respect to the rotation ϕ_y , and shear-torsional (ST) modes, where, on the contrary, ϕ_s can be neglected with respect to ϕ_y .

The same vibration modes have been considered here, particularly with regard to the influence of the external axisymmetric caps on them. Finally, the dependence of both lf and hf on the winding angle on the cylindrical central part, which can be an important parameter in the design of the aerospace vehicles vessels, has been considered.

Mathematical Model

A vessel shell profile is considered and a reference system s, y, z_s (Fig. 1), where s and y are oriented along the tangent to the cap

Received 12 April 2000; revision received 5 July 2000; accepted for publication 5 July 2000. Copyright © 2000 by Silvano Tizzi. Published by the American Institute of Aeronautics and Astronautics, Inc., with permission.

*Researcher, Aerospace Department.